Supporting Information for

Coalescing Cation Selectivity Approaches in Ionomers

Priyamvada Goyal, Ahmet Kusoglu*, and Adam Z. Weber*

***Corresponding Author: akusoglu@lbl.gov, azweber@lbl.gov**

Lawrence Berkeley National Laboratory, 1 Cyclotron Rd, Berkeley, CA 94720

SELECTIVITY MEASURES INTERCONVERSIONS

Table S1 lists the interconversions between selectivity measures from the five main sources identified from the Nafion literature.[1–11] The diagonal element (gray-shaded) represents the definition of the selectivity measure heading the respective columns. The other elements of the column convert from other selectivity measures [row header] to this diagonal element selectivity measure [column header]. For instance, second element in column 1 is converting the Steck selectivity, $S_{\mathrm{H}}^{\mathrm{C,St}}$ (row header) to the Okada selectivity, $S_{\mathrm{H}}^{\mathrm{C,Ok}}$ (column header).

Table S1. Expanded version of Table 3 in the main paper that explicitly lists all the interconversions among the chosen representative selectivity measures from Nafion literature. References: Okada and coworkers,[1–3] Steck,[4,5] Pintauro,[6–9] Hongsirikarn,[10] Crothers.[11]

	Okada, $S_{\mathrm{H}}^{\mathrm{C,Ok}} =$	Steck, $S_{\mathrm{H}}^{\mathrm{C,St}} =$	Pintauro, $S_{\mathrm{H}}^{\mathrm{C,Pin}} =$	Hongsirikarn, $S_{\mathrm{H}}^{\mathrm{C,Hon}} =$	Crothers, $S_{\mathrm{H}}^{\mathrm{C,Cr}} =$
$f(S_{\mathrm{H}}^{\mathrm{C,Ok}})$	$\left(\frac{x_{\mathrm{H}}^{\mathrm{m}}}{x_{\mathrm{H}}^{\mathrm{s}}}\right)^{\frac{z_{\mathrm{C}}}{z_{\mathrm{H}}}}\frac{x_{\mathrm{C}}^{\mathrm{s}}}{x_{\mathrm{C}}^{\mathrm{m}}}$	$\frac{1}{(S_{\mathrm{H}}^{\mathrm{C,Ok}})^{\frac{z_{\mathrm{H}}}{z_{\mathrm{C}}}}}\frac{\gamma_{\mathrm{H}}^{\mathrm{s}}/z_{\mathrm{H}}}{(\gamma_{\mathrm{C}}^{\mathrm{s}}/z_{\mathrm{C}})^{\frac{z_{\mathrm{H}}}{z_{\mathrm{C}}}}}(-z_{\mathrm{A}}c_{\mathrm{A}}^{\mathrm{s}})^{1-\frac{z_{\mathrm{H}}}{z_{\mathrm{C}}}}$	$\frac{1}{S_{\mathrm{H}}^{\mathrm{C,Ok}}}\left(\frac{x_{\mathrm{H}}^{\mathrm{m}}}{x_{\mathrm{H}}^{\mathrm{s}}}\right)^{\frac{z_{\mathrm{C}}}{z_{\mathrm{H}}}-1}$	$\frac{1}{S_{\mathrm{H}}^{\mathrm{C,Ok}}}\frac{(\Gamma x_{\mathrm{H}}^{\mathrm{s}})^{\frac{z_{\mathrm{C}}}{z_{\mathrm{H}}}}}{\Gamma x_{\mathrm{C}}^{\mathrm{s}}}$	$(S_{\mathrm{H}}^{\mathrm{C,Ok}})^{\frac{z_{\mathrm{H}}}{z_{\mathrm{C}}}}\left(\frac{z_{\mathrm{B}}y_{\mathrm{B}}^{\mathrm{m}}}{z_{\mathrm{A}}y_{\mathrm{A}}^{\mathrm{s}}}\right)^{1-\frac{z_{\mathrm{H}}}{z_{\mathrm{C}}}}$
$f(S_{\mathrm{H}}^{\mathrm{C,St}})$	$\frac{1}{(S_{\mathrm{H}}^{\mathrm{C,St}})^{\frac{z_{\mathrm{C}}}{z_{\mathrm{H}}}}}\frac{(\gamma_{\mathrm{H}}^{\mathrm{s}}/z_{\mathrm{H}})^{\frac{z_{\mathrm{C}}}{z_{\mathrm{H}}}}}{\gamma_{\mathrm{C}}^{\mathrm{s}}/z_{\mathrm{C}}}(-z_{\mathrm{A}}c_{\mathrm{A}}^{\mathrm{s}})^{\frac{z_{\mathrm{C}}}{z_{\mathrm{H}}}-1}$	$\frac{c_{\mathrm{H}}^{\mathrm{s}}\gamma_{\mathrm{H}}^{\mathrm{s}}}{x_{\mathrm{H}}^{\mathrm{m}}}\left(\frac{x_{\mathrm{C}}^{\mathrm{m}}}{c_{\mathrm{C}}^{\mathrm{s}}\gamma_{\mathrm{C}}^{\mathrm{s}}}\right)^{\frac{z_{\mathrm{H}}}{z_{\mathrm{C}}}}$	$(S_{\mathrm{H}}^{\mathrm{C,St}})^{\frac{z_{\mathrm{C}}}{z_{\mathrm{H}}}}\frac{\gamma_{\mathrm{C}}^{\mathrm{s}}/z_{\mathrm{C}}}{(\gamma_{\mathrm{H}}^{\mathrm{s}}/z_{\mathrm{H}})^{\frac{z_{\mathrm{C}}}{z_{\mathrm{H}}}}}\left(-z_{\mathrm{A}}c_{\mathrm{A}}^{\mathrm{s}}\frac{x_{\mathrm{H}}^{\mathrm{s}}}{x_{\mathrm{H}}^{\mathrm{m}}}\right)^{1-\frac{z_{\mathrm{C}}}{z_{\mathrm{H}}}}$	$(S_{\mathrm{H}}^{\mathrm{C,St}})^{\frac{z_{\mathrm{C}}}{z_{\mathrm{H}}}}(-z_{\mathrm{A}}c_{\mathrm{A}}^{\mathrm{s}})^{1-\frac{z_{\mathrm{C}}}{z_{\mathrm{H}}}}\frac{\frac{\gamma_{\mathrm{C}}^{\mathrm{s}}/z_{\mathrm{C}}}{\Gamma x_{\mathrm{C}}^{\mathrm{s}}}}{\left(\frac{\gamma_{\mathrm{H}}^{\mathrm{s}}/z_{\mathrm{H}}}{\Gamma x_{\mathrm{H}}^{\mathrm{s}}}\right)^{\frac{z_{\mathrm{C}}}{z_{\mathrm{H}}}}}$	$\frac{1}{S_{\mathrm{H}}^{\mathrm{C,St}}}\frac{\gamma_{\mathrm{H}}^{\mathrm{s}}/z_{\mathrm{H}}}{(\gamma_{\mathrm{C}}^{\mathrm{s}}/z_{\mathrm{C}})^{\frac{z_{\mathrm{H}}}{z_{\mathrm{C}}}}}(-z_{\mathrm{B}}c_{\mathrm{T}}^{\mathrm{s}}y_{\mathrm{B}}^{\mathrm{m}})^{1-\frac{z_{\mathrm{H}}}{z_{\mathrm{C}}}}$
$f(S_{\mathrm{H}}^{\mathrm{C,Pin}})$	$\frac{1}{S_{\mathrm{H}}^{\mathrm{C,Pin}}}\left(\frac{x_{\mathrm{H}}^{\mathrm{m}}}{x_{\mathrm{H}}^{\mathrm{s}}}\right)^{\frac{z_{\mathrm{C}}}{z_{\mathrm{H}}}-1}$	$(S_{\mathrm{H}}^{\mathrm{C,Pin}})^{\frac{z_{\mathrm{H}}}{z_{\mathrm{C}}}}\frac{\gamma_{\mathrm{H}}^{\mathrm{s}}/z_{\mathrm{H}}}{(\gamma_{\mathrm{C}}^{\mathrm{s}}/z_{\mathrm{C}})^{\frac{z_{\mathrm{H}}}{z_{\mathrm{C}}}}}\left(-z_{\mathrm{A}}c_{\mathrm{A}}^{\mathrm{s}}\frac{x_{\mathrm{H}}^{\mathrm{s}}}{x_{\mathrm{H}}^{\mathrm{m}}}\right)^{1-\frac{z_{\mathrm{H}}}{z_{\mathrm{C}}}}$	$\frac{c_{\mathrm{H}}^{\mathrm{s}}}{c_{\mathrm{H}}^{\mathrm{m}}}\frac{c_{\mathrm{C}}^{\mathrm{m}}}{c_{\mathrm{C}}^{\mathrm{s}}}$	$S_{\mathrm{H}}^{\mathrm{C,Pin}}\frac{(\Gamma x_{\mathrm{H}}^{\mathrm{s}})^{\frac{z_{\mathrm{C}}}{z_{\mathrm{H}}}}}{\Gamma x_{\mathrm{C}}^{\mathrm{s}}}\left(\frac{x_{\mathrm{H}}^{\mathrm{s}}}{x_{\mathrm{H}}^{\mathrm{m}}}\right)^{\frac{z_{\mathrm{C}}}{z_{\mathrm{H}}}-1}$	$\frac{1}{(S_{\mathrm{H}}^{\mathrm{C,Pin}})^{\frac{z_{\mathrm{H}}}{z_{\mathrm{C}}}}}\left(\frac{x_{\mathrm{H}}^{\mathrm{m}}}{x_{\mathrm{H}}^{\mathrm{s}}}\right)^{1-\frac{z_{\mathrm{H}}}{z_{\mathrm{C}}}}\left(\frac{z_{\mathrm{B}}y_{\mathrm{B}}^{\mathrm{m}}}{z_{\mathrm{A}}y_{\mathrm{A}}^{\mathrm{s}}}\right)^{1-\frac{z_{\mathrm{H}}}{z_{\mathrm{C}}}}$
$f(S_{\mathrm{H}}^{\mathrm{C,Hon}})$	$\frac{1}{S_{\mathrm{H}}^{\mathrm{C,Hon}}}\frac{(\Gamma x_{\mathrm{H}}^{\mathrm{s}})^{\frac{z_{\mathrm{C}}}{z_{\mathrm{H}}}}}{\Gamma x_{\mathrm{C}}^{\mathrm{s}}}$	$(S_{\mathrm{H}}^{\mathrm{C,Hon}})^{\frac{z_{\mathrm{H}}}{z_{\mathrm{C}}}}\frac{\frac{\gamma_{\mathrm{H}}^{\mathrm{s}}/z_{\mathrm{H}}}{\Gamma x_{\mathrm{H}}^{\mathrm{s}}}}{\left(\frac{\gamma_{\mathrm{C}}^{\mathrm{s}}/z_{\mathrm{C}}}{\Gamma x_{\mathrm{C}}^{\mathrm{s}}}\right)^{\frac{z_{\mathrm{H}}}{z_{\mathrm{C}}}}}(-z_{\mathrm{A}}c_{\mathrm{A}}^{\mathrm{s}})^{1-\frac{z_{\mathrm{H}}}{z_{\mathrm{C}}}}$	$S_{\mathrm{H}}^{\mathrm{C,Hon}}\left(\frac{x_{\mathrm{H}}^{\mathrm{m}}}{x_{\mathrm{H}}^{\mathrm{s}}}\right)^{\frac{z_{\mathrm{C}}}{z_{\mathrm{H}}}-1}\frac{\Gamma x_{\mathrm{C}}^{\mathrm{s}}}{(\Gamma x_{\mathrm{H}}^{\mathrm{s}})^{\frac{z_{\mathrm{C}}}{z_{\mathrm{H}}}}}$	$\left(\frac{x_{\mathrm{H}}^{\mathrm{s}}\Gamma x_{\mathrm{H}}^{\mathrm{s}}}{x_{\mathrm{H}}^{\mathrm{m}}}\right)^{\frac{z_{\mathrm{C}}}{z_{\mathrm{H}}}}\frac{x_{\mathrm{C}}^{\mathrm{m}}}{x_{\mathrm{C}}^{\mathrm{s}}\Gamma x_{\mathrm{C}}^{\mathrm{s}}}$	$\frac{1}{(S_{\mathrm{H}}^{\mathrm{C,Hon}})^{\frac{z_{\mathrm{H}}}{z_{\mathrm{C}}}}}\frac{\Gamma x_{\mathrm{H}}^{\mathrm{s}}}{(\Gamma x_{\mathrm{C}}^{\mathrm{s}})^{\frac{z_{\mathrm{H}}}{z_{\mathrm{C}}}}}\left(\frac{z_{\mathrm{A}}y_{\mathrm{A}}^{\mathrm{s}}}{z_{\mathrm{B}}y_{\mathrm{B}}^{\mathrm{m}}}\right)^{1-\frac{z_{\mathrm{H}}}{z_{\mathrm{C}}}}$
$f(S_{\mathrm{H}}^{\mathrm{C,Cr}})$	$(S_{\mathrm{H}}^{\mathrm{C,Cr}})^{\frac{z_{\mathrm{C}}}{z_{\mathrm{H}}}}\left(\frac{z_{\mathrm{A}}y_{\mathrm{A}}^{\mathrm{s}}}{z_{\mathrm{B}}y_{\mathrm{B}}^{\mathrm{m}}}\right)^{\frac{z_{\mathrm{C}}}{z_{\mathrm{H}}}-1}$	$\frac{1}{S_{\mathrm{H}}^{\mathrm{C,Cr}}}\frac{\gamma_{\mathrm{H}}^{\mathrm{s}}/z_{\mathrm{H}}}{(\gamma_{\mathrm{C}}^{\mathrm{s}}/z_{\mathrm{C}})^{\frac{z_{\mathrm{H}}}{z_{\mathrm{C}}}}}(-z_{\mathrm{B}}c_{\mathrm{T}}^{\mathrm{s}}y_{\mathrm{B}}^{\mathrm{m}})^{1-\frac{z_{\mathrm{H}}}{z_{\mathrm{C}}}}$	$\frac{1}{(S_{\mathrm{H}}^{\mathrm{C,Cr}})^{z_{\mathrm{C}}}}\left(\frac{x_{\mathrm{H}}^{\mathrm{m}}}{x_{\mathrm{H}}^{\mathrm{s}}}\right)^{\frac{z_{\mathrm{C}}}{z_{\mathrm{H}}}-1}\left(\frac{z_{\mathrm{B}}y_{\mathrm{B}}^{\mathrm{m}}}{z_{\mathrm{A}}y_{\mathrm{A}}^{\mathrm{s}}}\right)^{\frac{z_{\mathrm{C}}}{z_{\mathrm{H}}}-1}$	$\frac{1}{(S_{\mathrm{H}}^{\mathrm{C,Cr}})^{\frac{z_{\mathrm{C}}}{z_{\mathrm{H}}}}}\frac{(\Gamma x_{\mathrm{H}}^{\mathrm{s}})^{\frac{z_{\mathrm{C}}}{z_{\mathrm{H}}}}}{\Gamma x_{\mathrm{C}}^{\mathrm{s}}}\left(\frac{z_{\mathrm{B}}y_{\mathrm{B}}^{\mathrm{m}}}{z_{\mathrm{A}}y_{\mathrm{A}}^{\mathrm{s}}}\right)^{\frac{z_{\mathrm{C}}}{z_{\mathrm{H}}}-1}$	$\frac{y_{\mathrm{H}}^{\mathrm{m}}}{y_{\mathrm{H}}^{\mathrm{s}}}\left(\frac{y_{\mathrm{C}}^{\mathrm{s}}}{y_{\mathrm{C}}^{\mathrm{m}}}\right)^{\frac{z_{\mathrm{H}}}{z_{\mathrm{C}}}}$

Note on activity coefficients based on different composition measures

Activity coefficients based on one composition basis (γ_i), say molarity (c_i), can be converted to activity coefficients based on a different composition basis (Γ_i), say molality (m_i).[12] Recognizing that chemical potential can be equivalently described by two different composition measures and their associated activity coefficients,

$$\mu_i = RT\ln\gamma_i^{\theta} c_i\,\gamma_i = RT\ln\Gamma_i^{\theta}\, m_i\,\Gamma_i, \tag{S1}$$

where the standard chemical potentials are given by $\mu_i^{\theta,c} = RT\ln\gamma_i^{\theta}$ and $\mu_i^{\theta,m} = RT\ln\Gamma_i^{\theta}$. These standard state coefficients can be related by applying the primary reference condition that solutions behave ideally at dilution,

$$\Gamma_i^{\theta} = \rho_0\gamma_i^{\theta}. \tag{S2}$$

Combining equations (S1) and (S2) can yield a relationship between the activity coefficients as follows:

$$\boldsymbol{\Gamma_i = \frac{M_0 c_0}{\rho_0}\,\gamma_i.} \tag{S3}$$

Table S2 uses the same layout as Table S1 to express interconversions among selectivity coefficients based on different composition variables, namely molarity, molality, mole fraction, and cation fraction respectively in the order they appear in the table. Table S2 is aimed as a look-up table to allow processing of partitioning data in the most convenient formulation.

Table S2. Interconversions among selectivity measures based on major composition variables (superficial)

	$S_{\mathrm{H}}^{\mathrm{C,molar}} =$	$S_{\mathrm{H}}^{\mathrm{C,molal}} =$	$S_{\mathrm{H}}^{\mathrm{C,mole-fr}} =$	$S_{\mathrm{H}}^{\mathrm{C,cat-fr}} =$
$f(S_{\mathrm{H}}^{\mathrm{C,molar}})$	$\left(\frac{c_{\mathrm{H}}^{\mathrm{m}}}{c_{\mathrm{H}}^{\mathrm{s}}}\right)^{\frac{z_{\mathrm{C}}}{z_{\mathrm{H}}}} \frac{c_{\mathrm{C}}^{\mathrm{s}}}{c_{\mathrm{C}}^{\mathrm{m}}}$	$S_{\mathrm{H}}^{\mathrm{C,molar}} \left(\frac{c_0^{\mathrm{s}}}{c_0^{\mathrm{m}}}\right)^{\frac{z_{\mathrm{C}}}{z_{\mathrm{H}}}-1}$	$S_{\mathrm{H}}^{\mathrm{C,molar}} \left(\frac{c_{\mathrm{T}}^{\mathrm{s}}}{c_{\mathrm{T}}^{\mathrm{m}}}\right)^{\frac{z_{\mathrm{C}}}{z_{\mathrm{H}}}-1}$	$S_{\mathrm{H}}^{\mathrm{C,molar}} \left(\frac{z_{\mathrm{A}} c_{\mathrm{A}}^{\mathrm{s}}}{z_{\mathrm{B}} c_{\mathrm{B}}^{\mathrm{m}}}\right)^{\frac{z_{\mathrm{C}}}{z_{\mathrm{H}}}-1}$
$f(S_{\mathrm{H}}^{\mathrm{C,molal}})$	$S_{\mathrm{H}}^{\mathrm{C,molal}} \left(\frac{c_0^{\mathrm{m}}}{c_0^{\mathrm{s}}}\right)^{\frac{z_{\mathrm{C}}}{z_{\mathrm{H}}}-1}$	$\left(\frac{m_{\mathrm{H}}^{\mathrm{m}}}{m_{\mathrm{H}}^{\mathrm{s}}}\right)^{\frac{z_{\mathrm{C}}}{z_{\mathrm{H}}}} \frac{m_{\mathrm{C}}^{\mathrm{s}}}{m_{\mathrm{C}}^{\mathrm{m}}}$	$S_{\mathrm{H}}^{\mathrm{C,molal}} \left(\frac{y_0^{\mathrm{m}}}{y_0^{\mathrm{s}}}\right)^{\frac{z_{\mathrm{C}}}{z_{\mathrm{H}}}-1}$	$S_{\mathrm{H}}^{\mathrm{C,molal}} \left(\frac{z_{\mathrm{A}} m_{\mathrm{A}}^{\mathrm{s}}}{z_{\mathrm{B}} m_{\mathrm{B}}^{\mathrm{m}}}\right)^{\frac{z_{\mathrm{C}}}{z_{\mathrm{H}}}-1}$
$f(S_{\mathrm{H}}^{\mathrm{C,mole-fr}})$	$S_{\mathrm{H}}^{\mathrm{C,mole-fr}} \left(\frac{c_{\mathrm{T}}^{\mathrm{m}}}{c_{\mathrm{T}}^{\mathrm{s}}}\right)^{\frac{z_{\mathrm{C}}}{z_{\mathrm{H}}}-1}$	$S_{\mathrm{H}}^{\mathrm{C,mole-fr}} \left(\frac{y_0^{\mathrm{s}}}{y_0^{\mathrm{m}}}\right)^{\frac{z_{\mathrm{C}}}{z_{\mathrm{H}}}-1}$	$\left(\frac{y_{\mathrm{H}}^{\mathrm{m}}}{y_{\mathrm{H}}^{\mathrm{s}}}\right)^{\frac{z_{\mathrm{C}}}{z_{\mathrm{H}}}} \frac{y_{\mathrm{C}}^{\mathrm{s}}}{y_{\mathrm{C}}^{\mathrm{m}}}$	$S_{\mathrm{H}}^{\mathrm{C,mole-fr}} \left(\frac{z_{\mathrm{A}} y_{\mathrm{A}}^{\mathrm{s}}}{z_{\mathrm{B}} y_{\mathrm{B}}^{\mathrm{m}}}\right)^{\frac{z_{\mathrm{C}}}{z_{\mathrm{H}}}-1}$
$f(S_{\mathrm{H}}^{\mathrm{C,cat-fr}})$	$S_{\mathrm{H}}^{\mathrm{C,cat-fr}} \left(\frac{z_{\mathrm{B}} c_{\mathrm{B}}^{\mathrm{m}}}{z_{\mathrm{A}} c_{\mathrm{A}}^{\mathrm{s}}}\right)^{\frac{z_{\mathrm{C}}}{z_{\mathrm{H}}}-1}$	$S_{\mathrm{H}}^{\mathrm{C,cat-fr}} \left(\frac{z_{\mathrm{B}} m_{\mathrm{B}}^{\mathrm{m}}}{z_{\mathrm{A}} m_{\mathrm{A}}^{\mathrm{s}}}\right)^{\frac{z_{\mathrm{C}}}{z_{\mathrm{H}}}-1}$	$S_{\mathrm{H}}^{\mathrm{C,cat-fr}} \left(\frac{z_{\mathrm{B}} y_{\mathrm{B}}^{\mathrm{m}}}{z_{\mathrm{A}} y_{\mathrm{A}}^{\mathrm{s}}}\right)^{\frac{z_{\mathrm{C}}}{z_{\mathrm{H}}}-1}$	$\left(\frac{x_{\mathrm{H}}^{\mathrm{m}}}{x_{\mathrm{H}}^{\mathrm{s}}}\right)^{\frac{z_{\mathrm{C}}}{z_{\mathrm{H}}}} \frac{x_{\mathrm{C}}^{\mathrm{s}}}{x_{\mathrm{C}}^{\mathrm{m}}}$

COMPOSITION DEPENDENCE OF SELECTIVITY COEFFICIENTS: DIFFERENT REPORTING CONVENTIONS

The composition dependence of selectivity coefficients is clearly shown in Figure S1. All the plots are based on Okada's partitioning data. [1–3] For each combination of solution, $x_{\mathrm{H}}^{\mathrm{s}}$ and membrane proton fraction, $x_{\mathrm{H}}^{\mathrm{m}}$ a selectivity coefficient is calculated using the Okada measure, $S_{\mathrm{H}}^{\mathrm{C,Ok}}$ using the following expression:

$$S_{\mathrm{H}}^{\mathrm{C,Ok}} = \left(\frac{x_{\mathrm{H}}^{\mathrm{m}}}{x_{\mathrm{H}}^{\mathrm{s}}}\right)^{\frac{z_{\mathrm{C}}}{z_{\mathrm{H}}}} \frac{1 - x_{\mathrm{H}}^{\mathrm{s}}}{1 - x_{\mathrm{H}}^{\mathrm{m}}}. \tag{S4}$$

These selectivity values are plotted as the filled markers against the proton fraction in the membrane. Figure S1a displays the various ways in which different conventions can be used to report a single value of selectivity coefficient for the entire composition range through the specific example of the H^{+}/Li^{+} cation combination. The unfilled marker denotes the selectivity value reported by Okada and coworkers. [12–14] The horizontal dashed line is obtained by taking an average of all the pointwise selectivity values, in accordance with the Hongsirikarn convention.[10] The intersection of the vertical line at membrane proton fraction $x_{\mathrm{H}}^{\mathrm{m}} = 0.5$ and the curve (linear interpolation between two discrete filled markers) gives the selectivity value as defined by the Steck convention. [4,5]

Figures S1b and S1c respectively plot pointwise selectivity values vs membrane proton fraction for all the monovalent and multivalent cations, respectively, studied by Okada and coworkers, along with indicating the different selectivity values calculated based on the conventions defined in Figure S1a. The variation in selectivity with composition decreases for monovalent cations down the group, therefore leading to smaller differences in the single values obtained by the various conventions. Larger highly non-linear variation is observed for multivalent ions resulting in significantly different values from the three conventions; observe the vast difference between the unfilled marker, dashed horizontal line, and the point of intersection between the vertical line and selectivity curve denoted by a filled marker with a grey edge for different multivalent ions.

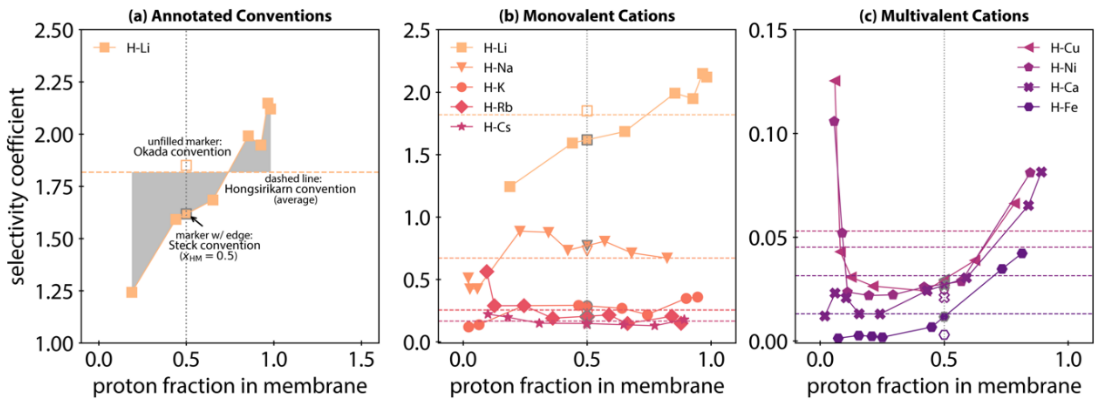

Figure S1. Composition dependence of selectivity coefficients along with a graphical comparison between single-valued selectivity coefficients obtained by using different reporting conventions (a) exposits via the H/Li combination how various conventions are demonstrated in the figure (b) and (c) apply the conventions from (a) to monovalent and multivalent cations, respectively, reported by Okada and coworkers.

Table S3 quantitatively summarizes the various ways of reporting selectivity coefficient values. To reiterate, all the calculations are based on Okada's measure but use different conventions to arrive at a single selectivity value. Values obtained by different methods diverge as the cation valence increases. For the divalent cations, the average convention (Hongsirkarn) consistently overpredicts selectivity, whereas the Steck convention values are fairly in agreement. The largest discrepancy is observed for the trivalent Fe^{3+}, where the Hongsirikarn and Steck approaches yield selectivity values that are an order of magnitude off from Okada's reported values. The data-fitting approach is the most successful in matching Okada's values across all valences.

Table S3. Comparison of selectivity coefficient reporting conventions

Ion/Ion Pair	Second cation valence	Reported (*Okada*)	Average (*Hongsirikarn* Convention)	at $x_{\mathrm{H}}^{\mathrm{m}} = 0.5$ (*Steck* Convection)	Non-linear fit (This work)
H/Li	1	1.850 ± 0.160	1.820	1.620	1.630
H/Na	1	0.730 ± 0.170	0.670	0.770	0.770
H/K	1	0.250 ± 0.060	0.250	0.290	0.270
H/Rb	1	0.200 ± 0.070	0.260	0.200	0.200
H/Cs	1	0.140 ± 0.070	0.170	0.150	0.150
H/Ca	2	0.021 ± 0.007	0.031	0.027	0.027
H/Cu	2	0.029 ± 0.010	0.052	0.029	0.039
H/Ni	2	0.025 ± 0.006	0.045	0.027	0.027
H/Fe	3	0.003 ± 0.002	0.012	0.013	0.003

CORRELATIONS AMONG FUNDAMENTAL PROPERTIES

A good quality correlation analysis requires the independent variables of the study to be as uncorrelated as possible. Several cation properties such as cation valence, z_{C}, ionic radius, r_{C},[15] charge density variables ($z_{\mathrm{C}}/r_{\mathrm{C}}$, $z_{\mathrm{C}}^2/r_{\mathrm{C}}$), hydrated ionic radius, $r_{\mathrm{C}}^{\mathrm{hyd}}$,[15] hydration enthalpy, $\Delta H_{\mathrm{C}}^{\mathrm{hyd}}$, [16] Lewis acid strength, $\mathrm{LAS}_{\mathrm{C}}$,[17,18] and electronegativity, χ_{C} [19,20] were identified as the relevant for the correlation analysis with cation selectivity. This section explores the correlations among these fundamental cation properties to select the appropriate independent variables for the selectivity correlation study.

Ion-solvent interactions: hydration enthalpy and hydrated radius

Hydration data (hydrated radius and hydration enthalpy) is fairly easily available for a large number of cations.[15,16] The heatmap in Figure S2 shows the strength of correlations between radius and hydration properties (values ranging from -1 and +1). Ionic radius, r_{C} does not directly correlate well with any hydration-like property on its own. In the heatmap, hydration enthalpy shows a very strong inverse correlation with the charge density variable $z_{\mathrm{C}}^2/r_{\mathrm{C}}$ across all valences. This correlation is based on the strong theoretical foundation of Born's hydration model.[21] Hydrated radius, similarly, shows an almost perfect correlation with the other charge density variable $z_{\mathrm{C}}/r_{\mathrm{C}}$. These correlations are verified by inspecting the scatterplots in Figure S3. Moreover, there is naturally a strong correlation between the two charge density variables themselves. In conclusion, given that it may be considerably easier to find valence and ionic radius of any cation, ionic radius, r_{C} and the charge density variable, $z_{\mathrm{C}}^2/r_{\mathrm{C}}$ are chosen as the independent variables from this group of properties.

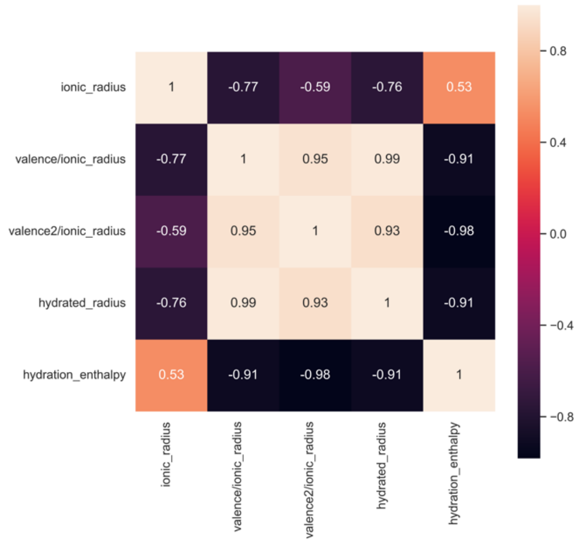

Figure S2. Heatmap of correlation coefficients among hydration-related cation fundamental properties

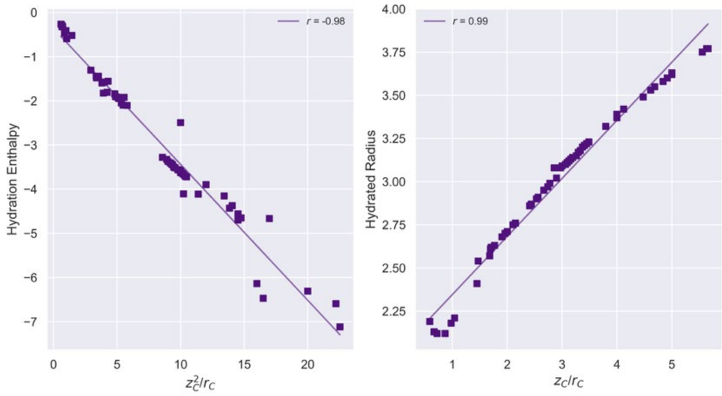

Figure S3. Scatter plots for hydration properties, hydration enthalpy and hydrated radius against charge density variables, $\boldsymbol{z_C^2/r_C}$ and $\boldsymbol{z_C/r_C}$.

Ion-ion interactions: electronegativity and Lewis acid strength

It is more challenging to obtain electronegativity and Lewis acid strength data from the literature as compared to the hydration data. However, this data was available for a large enough number of cations to draw definitive conclusions about collinearity.[17–20] The heatmap in Figure S4 shows that both electronegativity and LAS have moderately strong correlations with the charge density variables as well as with each other. The scatter plots in Figure S5 graphically confirm the strength of these correlations. Even though correlations for LAS and electronegativity aren't as perfect or indicative of "causation" as those for hydration enthalpy and hydrated radius, the coefficients of correlations are large enough to indicate strong multicollinearity among independent variables. Therefore, going ahead, ionic radius, $\boldsymbol{r_C}$ and charge density ($\boldsymbol{z_C^2/r_C}$) are the only independent variables retained.

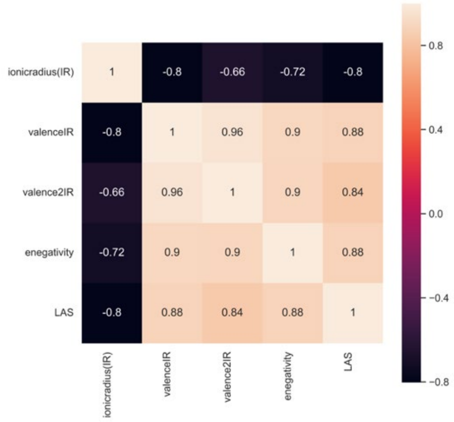

Figure S4. Heat map of electronegativity and LAS with other cation properties

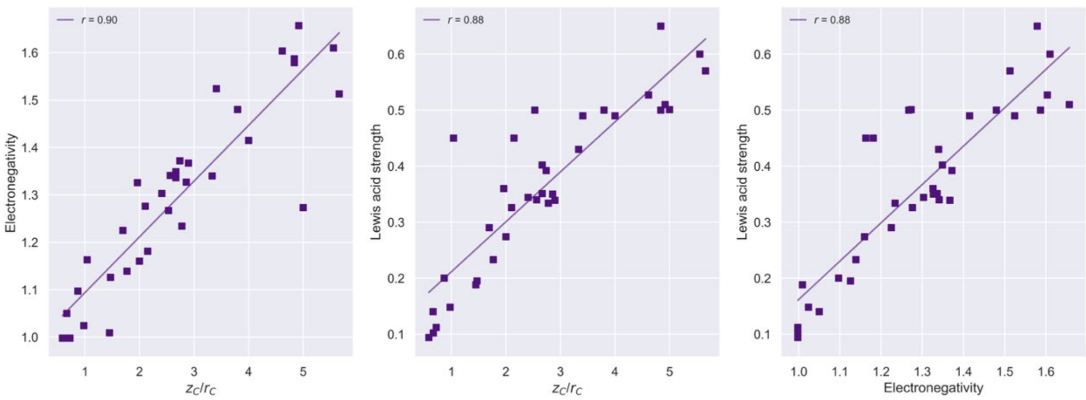

Figure S5. Scatter plots for electronegativity and Lewis strengths

CATION-CATION SELECTIVITY DATABASE: BEYOND PROTONS

Table S4. Sub-tables (a)–(d) produce the binary selectivity coefficients of Nafion membranes for Alkali metals Li, Na, K, and Cs relative to a host of other monovalent and divalent cations, respectively, from different sources across the literature. Although selectivities do not always follow an exact correlation with cation ionic radius, they are included to offer context of relative cation size.

(a)

Cation1	*Cation2*	*Cation2 Radius*	*Okada*[22]	*Pintauro*[6–9]	*Steck*[4]
Li^+	Cs^+	1.7	0.11	10.32	3.32
Li^+	Rb^+	1.49	0.17		2.79
Li^+	K^+	1.38	0.15	5.80	2.31
Li^+	Na^+	1.02	0.46	3.04	1.40
Li^+	Ag^+	1.15			1.30
Li^+	TEA^+	3.85		12.43	
Li^+	TMA^+	3.22		5.64	
Li^+	Ca^{2+}	1		6.96	
Li^+	Cu^{2+}	0.73		6.25	
Li^+	Ni^{2+}	0.69		5.47	
Li^+	Mg^{2+}	0.72		5.38	
Li^+	Pb^{2+}	1.18		5.16	
Li^+	Cd^{2+}	0.95		3.72	

(b)

Cation1	*Cation2*	*Cation2 Radius*	*Pintauro*[6]	*Zawodzinski*[23]	*Miyoshi*[24]	*Manning*[25]
Na^+	K^+	1.38		2.84	3.28	2.6
Na^+	TEA^+	3.58	11.13			
Na^+	TMA^+	3.22	4.58			
Na^+	Ca^{2+}	1			0.881	2.075
Na^+	Cu^{2+}	0.73			0.397	

(c)

Cation1	Cation2	Cation2 Radius	Pintauro[7–9]	Manning[25]
K^+	Cs^+	1.7	1.9	
K^+	Ca^{2+}	1	0.98	0.2
K^+	Cu^{2+}	0.73	0.89	
K^+	Ni^{2+}	0.69	0.74	
K^+	Mg^{2+}	0.72	0.71	
K^+	Pb^{2+}	1.18	0.78	
K^+	Cd^{2+}	0.95	0.56	

(d)

Cation1	Cation2	Cation2 Radius	Pintauro[6,7,9]
Cs^+	TEA^+	3.85	2.78
Cs^+	Ca^{2+}	1	0.53
Cs^+	Cu^{2+}	0.73	0.48
Cs^+	Ni^{2+}	0.69	0.44
Cs^+	Mg^{2+}	0.72	0.41
Cs^+	Pb^{2+}	1.18	0.36

NOTE: Some of the studies included above only shared the partitioning data without explicitly reporting selectivity values. We have computed selectivity values from their ion uptake data to create this database.

It is challenging to compare studies given the limited overlap in the cation combinations considered in the different studies. For the small overlap in alkali-alkali cations, interconversion between Pintauro and Okada measures yields satisfactory results. Steck selectivity values were not included in this interconversion due to the incomplete details regarding the computation of Li-alkali metal selectivity in that source.

Table S5. Selectivity coefficient values for alkali metals relative to Li as reported by Okada and Pintauro are produced along with the converted values from Pintauro to Okada convention. Given the possible differences in experimental conditions and reporting methods, the orders of magnitudes and trends are comparable. The last column reports the absolute relative error between the converted and reported selectivities according to the Okada measure.

Cation1	Cation2	Okada	Pintauro	Pintauro → Okada	Abs Relative Error
Li^+	Cs^+	0.11	10.32	0.097	0.28
Li^+	K^+	0.15	5.80	0.172	0.15
Li^+	Na^+	0.46	3.04	0.329	0.12

With the expanded database, it is also possible to examine whether a relation of the type

$$S_A^B = \frac{S_C^A}{S_C^B} \tag{S5}$$

can yield reliable binary selectivity coefficients. The formula was tested to obtain selectivities of alkali metals (B) relative to Li (A) by using their selectivity coefficients with protons (C).

Table S6. Equation 1 was employed to yield selectivity coefficients of alkali metals relative to Li by using the selectivity coefficients of the respective alkali metals and Li relative to protons. The calculated values are the same order of magnitude as the reported values and follow the same decreasing trend with alkali metal size. This exercise indicates that equation 1 may be used to generate approximate values of selectivity to temporarily extend the database in Table S4.

Cation1	*Cation2*	S_H^M	S_{Li}^M *(reported)*	S_{Li}^M *(calculated)*
H	Li	1.85		
Li	*Na*	0.73	0.46	0.3946
Li	*K*	0.25	0.15	0.1351
Li	*Rb*	0.2	0.17	0.1081
Li	*Cs*	0.14	0.11	0.0757

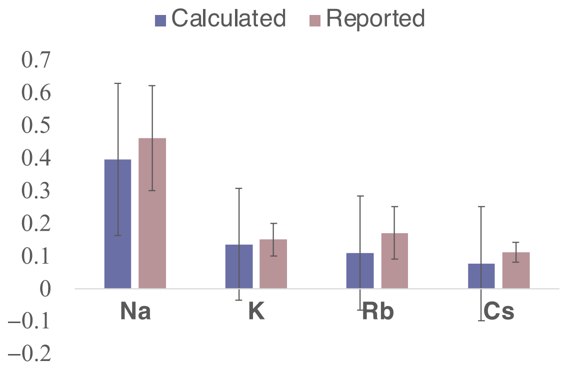

Figure S6. Selectivity values of alkali metals (Na, K, Rb, and Cs) relative to Li from the reported and calculated columns of Table 3 are compared via this bar plot.

References

1. Okada, T., Ayato, Y., Yuasa, M. & Sekine, I. The effect of impurity cations on the transport characteristics of perfluorosulfonated ionomer membranes. *Journal of Physical Chemistry B* **103**, 3315–3322 (1999).
2. Okada, T., Satou, H., Okuno, M. & Yuasa, M. Ion and water transport characteristics of perfluorosulfonated ionomer membranes with H+ and alkali metal cations. *Journal of Physical Chemistry B* **106**, 1267–1273 (2002).
3. Okada, T., Nakamura, N., Yuasa, M. & Sekine, I. Ion and Water Transport Characteristics in Membranes for Polymer Electrolyte Fuel Cells Containing H+ and Ca2+ Cations. *J Electrochem Soc* **144**, 2744–2750 (1997).
4. Yeager, H. L. & Steck, A. Ion-Exchange Selectivity and Metal Ion Separations with a Perfluorinated Cation-Exchange Polymer. *Anal Chem* **51**, 862–865 (1979).
5. Steck, A. & Yeager, H. L. Water Sorption and Cation-Exchange Selectivity of a Perfluorosulfonate Ion-Exchange Polymer. *Anal Chem* **52**, 1215–1218 (1980).
6. Palomo, J. & Pintauro, P. N. Competitive absorption of quaternary ammonium and alkali metal cations into a Nafion cation-exchange membrane. *J Memb Sci* **215**, 103–114 (2003).
7. Tandon, R. & Pintauro, P. N. Divalent/monovalent cation uptake selectivity in a Nafion cation-exchange membrane: Experimental and modeling studies. *J Memb Sci* **136**, 207–219 (1997).
8. Pintauro, P. N. & Bontha, J. R. Water orientation and ion solvation effect during multicomponent salt partitioning in a Nafion cation exchange membrane. *Chem Eng Sci* **49**, 3835–3851 (1994).
9. Pintauro, P. N., Tandon, R., Chao, L., Xu, W. & Evilia, R. Equilibrium partitioning of monovalent/bivalent cation-salt mixtures in nafion cation-exchange membranes. *Journal of Physical Chemistry* **99**, 12915–12924 (1995).
10. Hongsirikarn, K., Goodwin Jr, J. G., Greenway, S. & Creager, S. Effect of cations (Na+, Ca2+, Fe3+) on the conductivity of a Nafion membrane. *J Power Sources* **195**, 7213–7220 (2010).
11. Crothers, A. R., Darling, R. M., Kusoglu, A., Radke, C. J. & Weber, A. Z. Theory of Multicomponent Phenomena in Cation-Exchange Membranes: Part I. Thermodynamic Model and Validation. *J Electrochem Soc* **167**, 013547 (2020).

12. Okada, T., Nakamura, N., Yuasa, M. & Sekine, I. Ion and Water Transport Characteristics in Membranes for Polymer Electrolyte Fuel Cells Containing H + and Ca2 + Cations. *J Electrochem Soc* **144**, 2744–2750 (1997).
13. Okada, T., Satou, H., Okuno, M. & Yuasa, M. Ion and water transport characteristics of perfluorosulfonated ionomer membranes with H+ and alkali metal cations. *Journal of Physical Chemistry B* **106**, 1267–1273 (2002).
14. Okada, T., Ayato, Y., Satou, H., Yuasa, M. & Sekine, I. The effect of impurity cations on the oxygen reduction kinetics at platinum electrodes covered with perfluorinated ionomer. *Journal of Physical Chemistry B* **105**, 6980–6986 (2001).
15. Marcus, Y. Thermodynamics of Solvation of Ions. *Journal of Chemical Society Faraday Transactions* **87**, 2995–2999 (1991).
16. Smith, D. W. *Inorganic substances: a prelude to the study of descriptive inorganic chemistry*. *Choice Reviews Online* vol. 28 (Cambridge University Press, 1990).
17. Brown, I. D. What factors determine cation coordination numbers? *Acta Crystallographica Section B* **44**, 545–553 (1988).
18. Brown, I. D. & Skowron, A. Electronegativity and Lewis Acid Strength. *J Am Chem Soc* **112**, 3401–3403 (1990).
19. Li, K. & Xue, D. Estimation of electronegativity values of elements in different valence states. *Journal of Physical Chemistry A* **110**, 11332–11337 (2006).
20. Li, K., Li, M. & Xue, D. Solution-phase electronegativity scale: Insight into the chemical behaviors of metal ions in solution. *Journal of Physical Chemistry A* **116**, 4192–4198 (2012).
21. Latimer, W. M., Pitzer, K. S. & Slansky, C. M. The Free Energy of Hydration of Gaseous Ions, and the Absolute Potential of the Normal Calomel Electrode. *J Chem Phys* **7**, 485–489 (1939).
22. Okada, T., Arimura, N., Satou, H., Yuasa, M. & Kikuchi, T. Membrane transport characteristics of binary cation systems with Li + and alkali metal cations in perfluorosulfonated ionomer. *Electrochim Acta* **50**, 3569–3575 (2005).
23. Peng, J., Tian, M., Cantillo, N. M. & Zawodzinski, T. The ion and water transport properties of K+ and Na+ form perfluorosulfonic acid polymer. *Electrochim Acta* **282**, 544–554 (2018).
24. Miyoshi, H., Yamagami, M. & Kataoka, T. Influence of the Concentration of Ions in Solution on the Partition Coefficient between Cation Exchange Membrane and Solution. *Solvent Extraction and Ion Exchange* **11**, 505–520 (1993).
25. Manning, M. J. & Meleheimer, S. S. Binary and Ternary Ion-Exchange Equilibria with a Perfluorosulfonic Acid Membrane. *Industrial and Engineering Chemistry Fundamentals* **22**, 311–317 (1983).